Sub-electron-volt chemical shifts and strong interference effects measured in the resonance x-ray scattering spectra of aniline

Yi Luo and Hans Ågren
Institute of Physics and Measurement Technology, Linköping University, S-58183, Linköping, Sweden

Jinghua Guo, Per Skytt, Nial Wassdahl, and Joseph Nordgren
Department of Physics, Uppsala University, Box 530, S-75121 Uppsala, Sweden
(Received 17 April 1995)

By exploring the monosubstituted benzene compound aniline, we demonstrate that resonance inelastic x-ray spectroscopy of chemically shifted species is *site selective*. Core-excited levels with distinct, super-electron-volt shifts can be resonantly excited and their x-ray emission spectra analyzed separately. Core-excited levels referring to sites with small, sub-electron-volt, chemical shifts give resonant x-ray spectra that interfere strongly. It is demonstrated that this interference, which is manifested in the one-step model, can be used to monitor chemical shifts in the sub-electron-volt energy region. We show that in the limit when these chemical shifts go to zero some salient symmetry-selective features of the benzene resonant x-ray emission spectrum are restored in the aniline spectra.

PACS number(s): 33.20.Rm, 33.70.−w

I. INTRODUCTION

The influence of the chemical or physical state of the element on x-ray emission spectra was discovered in the 1920s [1], thereby refuting the idea that an x-ray spectrum is the property of the element only. The *chemical shifts* of core-to-core radiative transitions in the hard x-ray wavelength region have since then become well characterized and the underlying mechanism basically understood [2]. In the soft x-ray wavelength region the x-ray transitions connect penultimate core levels with valence levels and are therefore strongly influenced by the chemical environment in terms of electronic and geometrical structures given as *molecular* properties. With modern spectrometers it has been possible to monitor such influences both on a molecular orbital and a vibronic level of energy resolution. However, nonresonant x-ray spectra excited by broadband photons involve excitations of all core-shifted states, and the decay spectra from these shifted states become completely mixed in the final spectrum.

The capability of recent synchrotron radiation techniques to utilize small band passes at high energies in the soft x-ray region has opened the prospect to exclusively excite shifted core-excitation levels, and thus to investigate the role of core level shifts also in molecular valence x-ray spectra. In the present work we use aniline to demonstrate this feature. Moreover, as we also demonstrate here, the resonantly excited x-ray emission spectra referring to core levels shifted within the sub-electron-volt range will be strongly dependent on interference effects. These in turn are dependent on the precise values of the chemical shifts, and even very small such shifts, far smaller than the resolution limit in the corresponding core absorption spectra, give rise to significant changes in the spectra. We show that as the chemical shifts progressively become smaller, some salient symmetry-dependent features of the degenerate system are restored, here implying that much of the benzene resonant x-ray emission spectrum is restored in the aniline spectra. Due to these particular interference effects the one- and two-step model descriptions of the resonance x-ray emission phenomenon differ strongly, and only the former is warranted for investigations of spectra referring to core-excited resonant states with small chemical shifts.

II. EXPERIMENT

The experiments were performed at beamline 7.0 of the Advanced Light Source (ALS), Lawrence Berkeley Laboratory (LBL) [3]. This beamline comprises a 5-meter, 5-cm-period undulator and a 10.000-resolving-power spherical grating monochromator (SGM) covering the spectral range from 100 to 1300 eV. Condensed aniline was obtained by dosing the sample gas onto a liquid nitrogen cooled Cu metal surface. The temperature of the Cu metal was about −160 °C during the whole experimental period. The aniline film was very thick as inferred from its visible color. The sample liquid was purified by a freeze-pump sequence prior to exposure. The soft x-ray fluorescence was recorded in the polarization plane, and normal to the incident photon beam using a high-resolution grazing-incidence grating spectrometer with a two-dimensional detector [4]. The sample was oriented so that the incident photon beam impinged at an angle of 60° relative to the surface normal, in order to suppress effects due to self-absorption. The bandpass of the incident photon beam was set to 0.22 eV in the emission measurements, and the fluorescence spectrometer resolution was 0.45 eV. The energy scale of the x-ray emission spectra was calibrated by using the elastic peak and Cu metal $L_{II,III}$ emission lines recorded in the third order of diffraction. The spectra are shown in Fig. 1.

III. METHOD

The analysis of the resonant inelastic x-ray scattering requires in general a one-step theoretical formalism, which leads to a Kramers-Heisenberg-type dispersion formula for

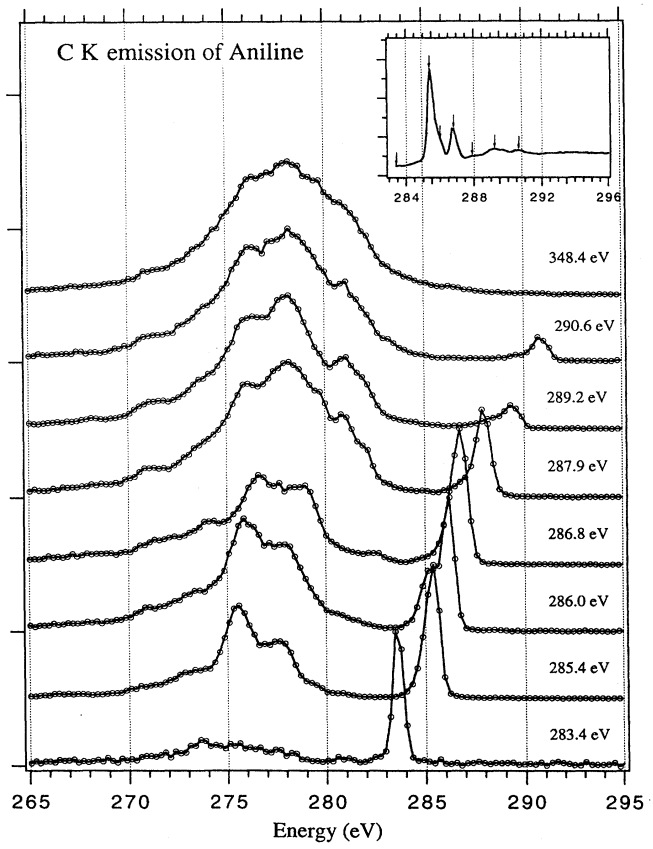

FIG. 1. RIXS spectra of aniline obtained with various photon excitation energies marked in the inset with the corresponding x-ray-absorption spectrum.

the cross section. General theory for resonant x-ray emission spectra, also called resonant inelastic and elastic x-ray scattering spectra (RIXS and REXS), of randomly oriented molecules has been presented in our recent studies [5–7]. The consequence of this theory for molecules with fixed orientation has also been given [7].

A. Interference

For a general account of the underlying theory we refer to the papers quoted above. Here we focus on the interference effect because it is crucial for the understanding of the chemically shifted RIXS spectra, and make an illustration of this effect by a simple four-state model that has a direct connection with the RIXS spectra of the aniline molecule studied here. We consider two core orbitals (k_1,k_2), one occupied π orbital (n) and one unoccupied π^* orbital (ν) in C_{2v} symmetry. The dipole transition moments between core orbitals and the unoccupied orbital and the occupied orbital are denoted as $d^z_{\nu k_i}$ and $d^z_{nk_i}$, $(i=1,2)$, respectively. In the one-step model (OS) the emission intensity is

$$\sigma^{\mathrm{OS}}(\omega',\omega_0)\propto\sigma_1+\sigma_2+\sigma_{\mathrm{int}} \tag{1}$$

and

$$\sigma_1=\frac{D_{k_1}^2}{\Delta_{k_1}^2+\Gamma^2},\quad \sigma_2=\frac{D_{k_2}^2}{\Delta_{k_2}^2+\Gamma^2},$$

$$\sigma_{\mathrm{int}}=2D_{k_1}D_{k_2}\frac{\Delta_{k_1}\Delta_{k_2}+\Gamma^2}{(\Delta_{k_1}^2+\Gamma^2)(\Delta_{k_2}^2+\Gamma^2)}, \tag{2}$$

where $D_{k_i}=\alpha\omega_{\nu k_i}\omega_{nk_i}(\nu)d^z_{\nu k_i}d^z_{nk_i}$ is defined as the transition strength of channel i. $\Delta_{k_i}=\omega'-\omega_{nk_i}$. The lifetimes of the two core-excited states are assumed to be the same. According to the general two-step model (TSg) [7], the emission intensity is

$$\sigma^{\mathrm{TSg}}(\omega',\omega_0)\propto\sigma_1+\sigma_2. \tag{3}$$

To rewrite Eq. (2) one has

$$\sigma^{\mathrm{OS}}(\omega',\omega)\propto(\sigma_1+\sigma_2)(1+I_{\mathrm{int}}) \tag{4}$$

and

$$I_{\mathrm{int}}=\frac{D_{k_1}D_{k_2}(\Delta_{k_1}\Delta_{k_2}+\Gamma^2)}{D_{k_1}^2(\Delta_{k_2}^2+\Gamma^2)+D_{k_2}^2(\Delta_{k_1}^2+\Gamma^2)}. \tag{5}$$

The difference between the one-step and the two-step models is thus dependent on the interference strength I_{int}, $0\leq|I_{\mathrm{int}}|\geq 1$. If the interference strength is equal to zero, both models will give the same result. This holds only for two cases, first when there is only one channel available, i.e., when D_{k_1} or D_{k_2} is zero, and second, when $\Delta_{k_1}\Delta_{k_2}=-\Gamma^2$, which indicates that one could manipulate the interference pattern by detuning the excitation energy. When I_{int} is equal to -1, the spectral line of emission would be totally absent.

Using a very narrow incoming beam it is possible to tune the excitation energy exactly resonant with one core-excited state. We thus assume that $D_{k_1}=0$, i.e., the excitation energy is resonant with the $k_1^{-1}\pi^*$ state. Therefore, the interference strength is

$$I_{\mathrm{int}}=\frac{2R_d}{1+R_\omega^2+R_d^2}, \tag{6}$$

where $R_d=D_{k_2}/D_{k_1}$, the ratio between the transition strength of the near-resonant channel and that of the resonant channel. $R_\omega=\delta\omega_{21}/\Gamma$ and $\delta\omega_{21}=E(k_2^{-1}\nu)-E(k_1^{-1}\nu)$, the energy difference between two core-excited states. For fixed transition strengths of the two channels, the maximum interference strength occurs at $R_\omega=0$ when the two core-excited states are degenerate. When the energy difference between the two core-excited states is unchanged, the maximum interference strength corresponds to the condition that $R_d=(1+R_\omega^2)^{1/2}$.

By considering vibrational excitations it is quite easy to fulfill the condition that $R_\omega=0$ even for two well separated core-excited states. In this case, the energy differences between core-excited states are no longer represented by the electronic transition energies; instead, one should consider the energy differences between vibrational levels of the core-excited states. Similar considerations should also be applied for the transition strengths of two channels.

B. Computations

In addition to the resonant x-ray emission spectra of aniline, we have also computed the nonresonant emission and the absorption spectra of this molecule. The assignment of the latter spectrum is crucial in order to understand the resonant emission spectra of interest here. We have focused on the strong absorption features located at the low-energy part of this spectrum, and which, as we find here, all are composed of resonant excitations to the first π^* level. This part is thus composed of $C_i \rightarrow \pi^*$ $(i=1,2,3,4)$ transitions from the four different shifted carbon core sites. As we have discussed in the preceding section, the energy differences between different core-excited states are very important for the quantitative description of the RIXS process. The absorption part of the RIXS process is investigated by using static exchange [8] and multiconfigurational self-consistent (MCSCF) [9] methods, invoking relaxation and correlation effects. Extended basis sets (augmented double and triple ζ) have been employed, which, based on previous experience with absorption [8] and emission [7,10,11] spectra, should be well sufficient. We point out that the obtained shifts actually are supported both by the absorption and the emission spectra, as further explained in the following sections.

We use canonical Hartree-Fock theory for orbital energies and transition moments in the emission part (nonresonant and resonant). This level of theory has been qualified earlier on many occasions both for large and small molecules [7,10,11]. A factor of 1.3 has been used to compress the width of the total valence band. The need for this measure follows from the fact that Hartree-Fock calculations generally exaggerate the total width of the valence band due to the neglect of electron correlation (see Ref. [7] and references therein).

The lifetime widths of the core-excited states are assumed to be identical; $\Gamma=0.15$ eV (equaling the lifetime width for the first carbon core-excited state of CO_2 measured by electron energy loss spectroscopy [12]). The present analysis is restricted to the pure resonant part of the scattering process, assuming randomly oriented aniline molecules and detection and polarization directions as described in the experimental section.

IV. RESULTS AND DISCUSSION

The RIXS spectra of aniline recorded at various excitation energies are given in Fig. 1 together with the absorption spectrum, on which the excitation energies are indicated (see inset of Fig. 1). A salient feature in these spectra is the high-energy recombination peaks (elastic peaks). These will, however, not be considered in the present work (see Refs. [13—15] for some general properties of elastic x-ray scattering). Except for the nonresonant spectrum (Fig. 2), we will focus on the resonant inelastic spectra for the low energies corresponding to the two strong resonances in the x-ray absorption spectrum, see Fig. 3. Higher resonant spectra, at 287.9 eV and up, become rather nonresonant like. It is relevant to start out a discussion of the resonant inelastic scattering spectrum of aniline by analyzing the near-edge core absorption and the nonresonant x-ray spectra first.

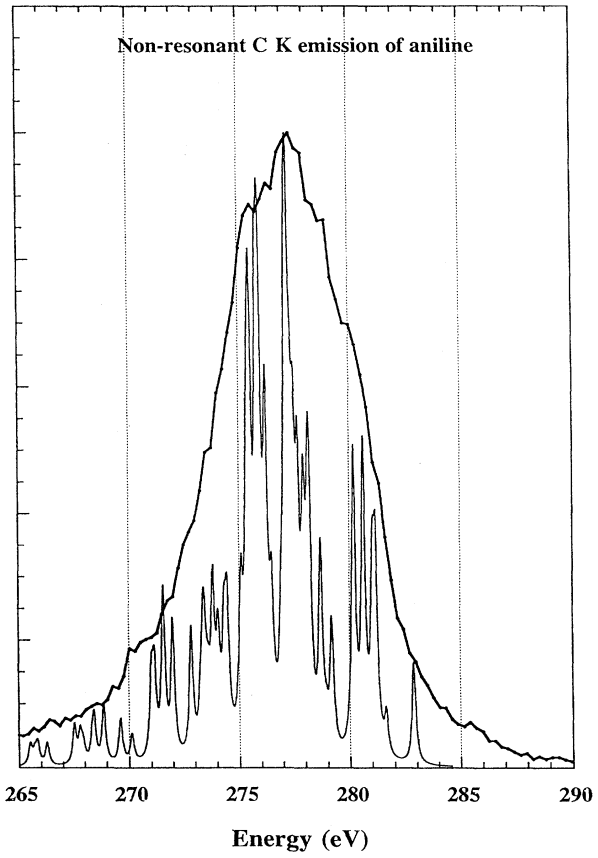

FIG. 2. Calculated and experimental nonresonant x-ray emission spectrum of aniline.

A. The nonresonant x-ray emission spectrum of aniline

We have employed the conventional two-step model for the calculations of the nonresonant spectrum of aniline. The calculated spectrum is shown together with the corresponding experimental spectrum in Fig. 2. Note that the distribution of the final valence hole states is obtained well in line with that given by UPS data [16] (after compression, see computational section). In the nonresonant spectrum generated by electron impact six features can be distinguished [16], which correspond well to the grouping of intensities predicted by the present calculations, both intensitywise and energywise. It can be noted that the full transition moments reproduce the spectral trends better than the one-center decomposition analysis, in particular a better balance of intensity between high- and low-energy parts is obtained.

Due to the amino substitution the benzene symmetry D_{6h} is lowered to C_{2v} for aniline. The core orbitals for the latter molecule can be represented as $C_1(a_1)$, $C_2(a_1,b_2)$, $C_3(a_1,b_2)$, and $C_4(a_1)$, using the order of the C atoms (C_i) given in the inset of Fig. 3. Unlike benzene, some core orbitals of aniline are nondegenerate, in particular, the $C_1(a_1)$ core orbital is well separated. For a given occupied orbital n, emission lines referring to the core orbitals k_i located at the different carbon atoms (C_i) can be observed (with separate energies denoted $\omega' = \omega_{nk_i}$). This gives a superposition of different core-sited spectra, and hence com-

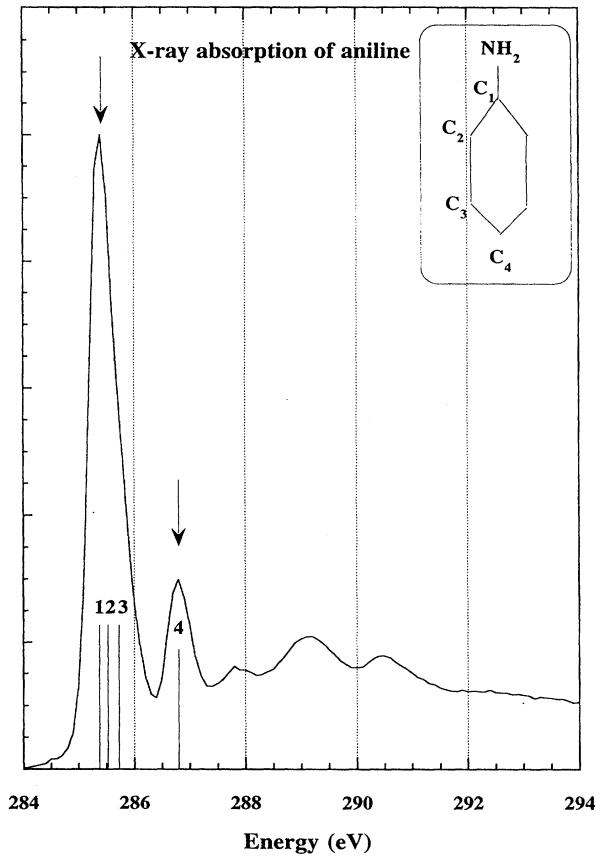

FIG. 3. x-ray-absorption spectrum of aniline. The corresponding assignments in the spectrum are (1) $C_2(a_1)\pi^*(b_1)$, (2) $C_3(a_1)\pi^*(b_1)$, (3) $C_4(a_1)\pi^*(b_1)$, and (4) $C_1(a_1)\pi^*(b_1)$.

plex unresolved features in comparison with the more degenerate benzene molecule, or with respect to the substituent nonresonant spectrum, here the amino N K spectrum [16]. On the other hand, with energy selective excitation, nonoverlapping emission spectra can be obtained even for species with core level shifts, as discussed further below.

B. The core absorption spectrum of aniline

The NEXAFS (near-edge core absorption) spectrum of aniline shows some similarities with that of benzene [17–19]. In the discrete part the latter contains only one large resonance, the $\pi^*(e_{2u})$ level, with three weak σ excitations and a fairly weak second π^* excitation at the threshold. We find the aniline spectrum to be dominated by the first π^* level, which now is represented by two strong bands in the spectrum, the first containing the three C_2-, C_3-, and C_4-π^* transitions grouped at about 285.4 eV and the second with the C_1-π^* transition located at 286.8 eV. This could be understood by the fact that the appearance of the NH_2 group splits the core orbitals of the carbon atoms, and also lifts the degeneracy of the $\pi^* e_{2u}$ molecular orbital (MO) of benzene. The first unoccupied e_{2u} orbital thus splits into two orbitals, b_1 and a_2. Likewise is the outermost occupied e_{1g} orbital, which refers to the strong outermost band in the nonresonant emission, and which becomes symmetry forbidden in the resonant lowest unoccupied molecular orbital (LUMO) (e_{2u}) emission spectrum of benzene [20], split into b_1 and a_2 orbitals for aniline. As predicted in Ref. [21], a significant σ charge donation from the phenyl to the amino group takes place, which, however, to a large degree is balanced by a donation the other way in the π system (conjugative effect). The net effect is a negative charging of the amino group (0.11 electrons [21]) which by virtue of the potential model [22] should lead to an increased ionization potential for the carbon site, here C_1, that loses charge to the amino group. We find that the other sites follow an alternate behavior for the core hole shifts.

Transitions from the core orbitals with symmetry a_1 to the $\pi^*(a_2)$ molecular orbital are not allowed. Although transitions from $C_2(b_2)$ and $C_3(b_2)$ to the $\pi^*(a_2)$ orbital are allowed, their intensities are found to be quite weak. The static exchange calculations show that the absorption intensities to the $\pi^*(b_1)$ level are of the same order of magnitude for the four core excitations. The magnitude of the shifts for the core-to-π^* excitations differs from that of the bare core hole states, in that they are now more compressed, especially the shifts between the C_2-, C_3-, and C_4-to-$\pi^*(b_1)$ levels become small. The MCSCF calculations, in which both relaxation and correlation effects are taken into account, indicate that the lowest core-excited state is the $C_3(a_1)\pi^*(b_1)$ state, but

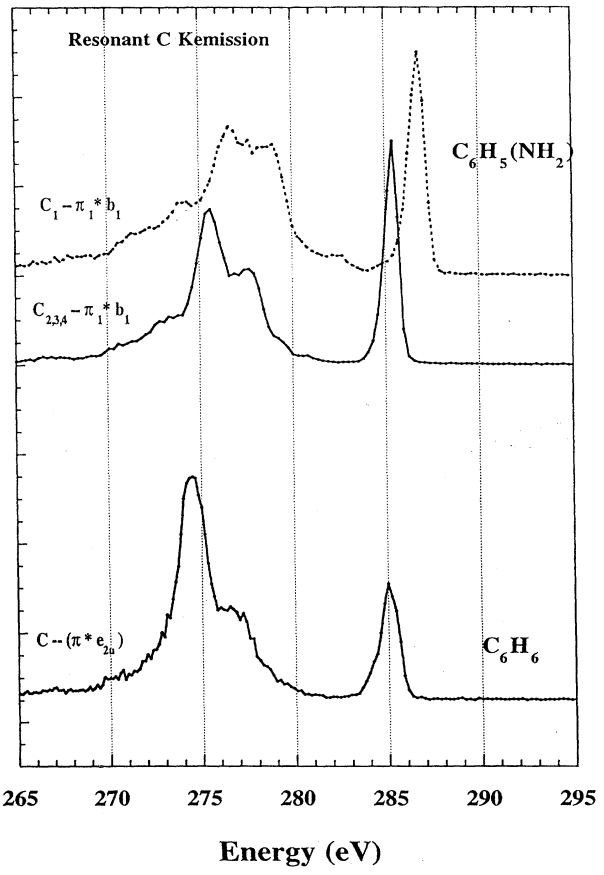

FIG. 4. Resonant x-ray emission spectra of benzene and aniline recorded at excitation energies resonant with the lowest π^* levels.

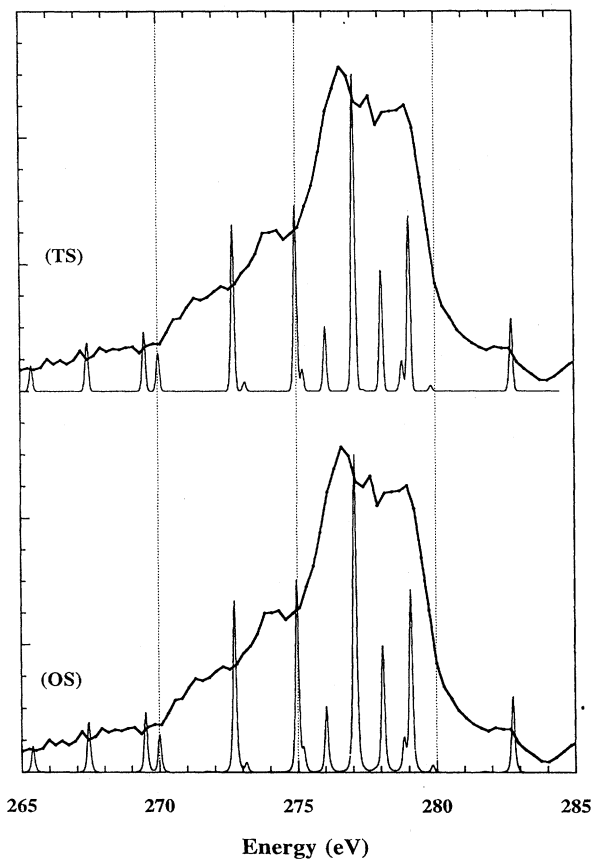

FIG. 5. Experimental and calculated resonant x-ray emission spectra of aniline for the $C_1(a_1)-\pi^*b_1$ excitation. Comparison of one-step (OS) and two-step (TS) models.

that it is almost degenerate with the core-excited $C_2(a_1)\pi^*(b_1)$ state. The π complete active space, large basis set, calculation gives an energy of only 0.03 eV for this energy difference, and energy shifts with respect to $C_3(a_1)\pi^*(b_1)$ of 0.29 eV for the $C_4(a_1)\pi^*(b_1)$ level and of 1.15 eV for the $C_1(a_1)\pi^*(b_1)$ level. This leads to an assignment of the first resonance centered at 285.4 eV to transitions from the $C_{2,3,4}$ core orbitals to the first $\pi^*(b_1)$ molecular orbital. The second resonance is assigned to transitions from the C_1 carbon to the first $\pi^*(b_1)$ molecular orbital. This assignment of the aniline NEXAFS spectrum is different from the previous one given by Solomon *et al.* [23] based on the SCF-MO calculations, but accords well with the new high-resolution NEXAFS spectrum given in Fig. 3. In particular, the narrow but intensive 285.4 eV feature (predicted energy difference of 0.3 eV), and the 1.4 eV splitting with the second π^* resonance (predicted to 1.2 eV) are well accounted for. Although core energy shifts are expected to be much better reproduced than absolute transition energies by ΔMCSCF and ΔSCF procedures [24], one must keep an attitude of reserve against such exceedingly small energies. However, except for the NEXAFS spectrum, also the RIXS spectra of aniline support the smallness of the shifts, which, as discussed below, can be monitored by the interference effects they induce.

C. The resonant x-ray emission spectra of aniline

The resonant x-ray emission spectra of aniline corresponding to the first two $\pi^*(b_1)$ resonances in the x-ray absorption spectrum are presented in Fig. 4. For comparison, the resonant x-ray emission spectrum of benzene referring to to the first $\pi^*(e_{2u})$ resonance is also included in this figure. One finds the extraordinary feature that when the excitation energy is tuned resonant with the first π^* band (referring to the compound $C_{2,3,4}\pi^*$ levels for aniline), the two molecules show quite similar x-ray emission spectra. The absence of intensity in the 280–284 eV energy region is noteworthy, since this is the result of the strict parity selection rule for RIXS applied to D_{6h} benzene [20]. By lowering the symmetry from D_{6h} (benzene) to C_{2v} (aniline), the parity selection rule no longer holds. On this ground one expects that the intensity should be observed in the of 280–284 eV energy region for aniline. This is actually the case when the excitation energy is resonant to the second π^* resonance ($C_1(a_1)\pi^*(b_1)$). The two resonant x-ray emission spectra shown in Fig. 4 possess the same initial and final states but different intermediate states. This indicates that multichannel

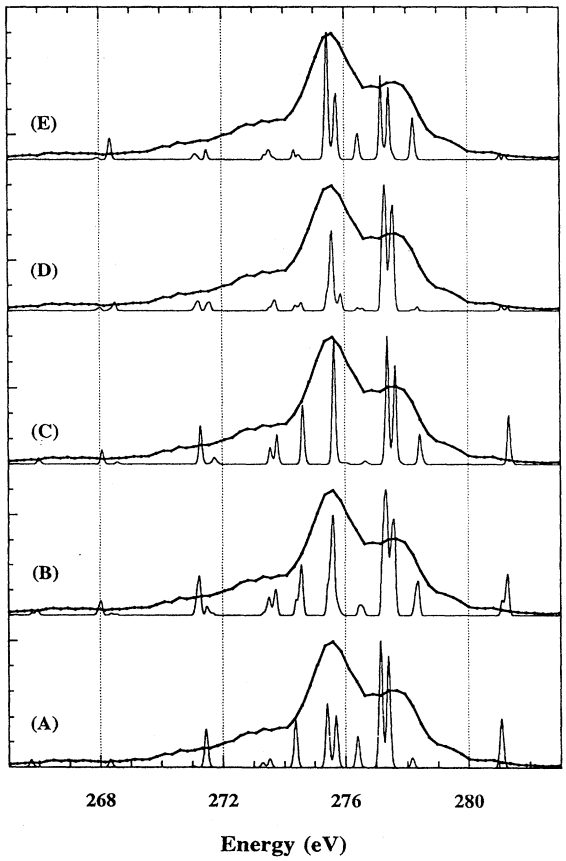

FIG. 6. Calculated resonant x-ray spectra referring to $C_{2,3,4}-\pi^*b_1$ resonances using different chemical shifts. The experimental spectrum is shown for comparison. One transition channel $C_2-\pi^*b_1$ (a). Two transition channels, $C_{2,4}-\pi^*b_1$: $\delta_{2,4}=0.3$ eV (b). Three transition channels, $C_{2,3,4}-\pi^*b_1$: $\delta_{2,3}=0.5$ eV (c); $\delta_{2,3}=0.2$ eV (d); $\delta_{2,3}=0.05$ eV (e).

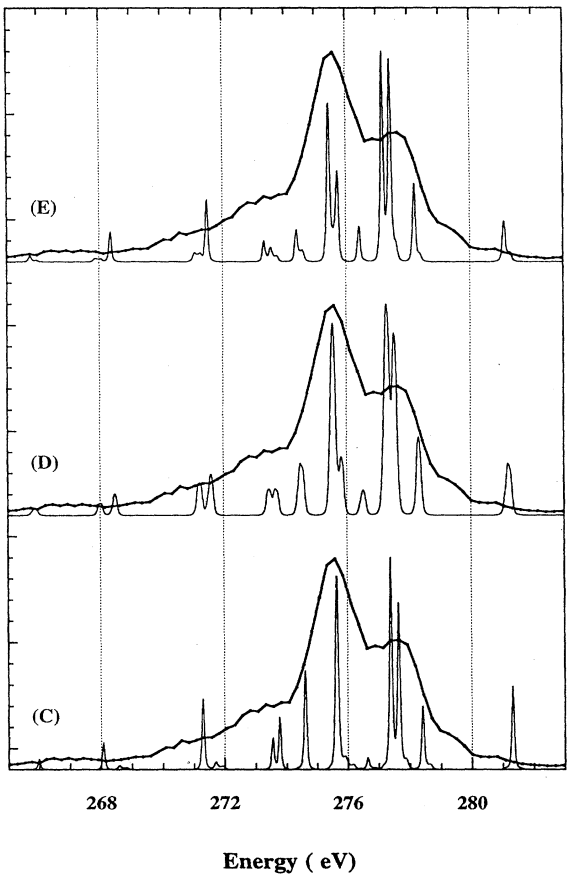

FIG. 7. The same conditions as for Fig. 6, but with calculations based on the two-step model.

interference should be responsible for the absence of the intensity in the 280–284 eV energy region for the first, compound, π^* resonance of aniline.

Since the second π^* resonance of aniline is dominated by only one channel, $C_1(a_1)\pi^*(b_1)$, the interference effect should be negligible. Spectra calculated by the one- and two-step models are accordingly almost the same, see Fig. 5. These spectra also accord well with the experimental spectrum shown in Fig. 4. However, for the spectrum referring to the first compound π^* resonance of aniline, three different channels, labeled in Fig. 3, should be taken into account. Due to the small energy separations among those three intermediate core-excited states, especially between $C_3(a_1)\pi^*(b_1)$ and $C_2(a_1)\pi^*(b_1)$, the interference effect is expected to be large as discussed in Sec. III A.

We simulate here the interference effect in some detail using the one-step model: The MCSCF value of 0.3 eV for the energy difference between the $C_3(a_1)\pi^*(b_1)$ and $C_4(a_1)\pi^*(b_1)$ levels is used: The energy difference between the $C_3(a_1)\pi^*(b_1)$ and $C_2(a_1)\pi^*(b_1)$ levels is labeled δ_{23}; the spectra for different values of δ_{23} (from 0.05 eV to 0.5 eV) are illustrated in Fig. 6. The relation between the energy difference and interference effect is clearly displayed by this figure. For comparison, two simulated spectra considering a single channel, the $C_2(a_1)\pi^*(b_1)$ channel, and two channels, the $C_{2,4}(a_1)\pi^*(b_1)$ channels, are also shown. These results show that when the δ_{23} shift gets smaller, the agreement with the experimental spectrum gets better, and that the intensity distribution is crucially dependent on the interference effect. By fully considering this effect, not only is the absence of the intensity in the energy region of 280–284 eV explained, but the correct intensity distribution for the whole spectrum is also obtained. The spectra have also been simulated with the two-step model using the same parameters, see Fig. 7. A quite poor agreement with the experimental spectrum is then obtained for all values of δ_{23}. This is mainly due to the fact that the interference effects are neglected by the two-step model. The large differences between the two models are illustrated in Fig. 8. It is quite evident that the two-step model simply cannot be used for spectra where more than one dominant channel is involved in the resonant x-ray emission process, as is the case for species with small chemical shifts.

V. SUMMARY

The purpose of the present work was to investigate the site dependency of resonant x-ray emission spectra, and to explore to what degree chemical shifts of core levels are reflected in such spectra. The aniline molecule was used for this purpose. Although we have investigated just this one

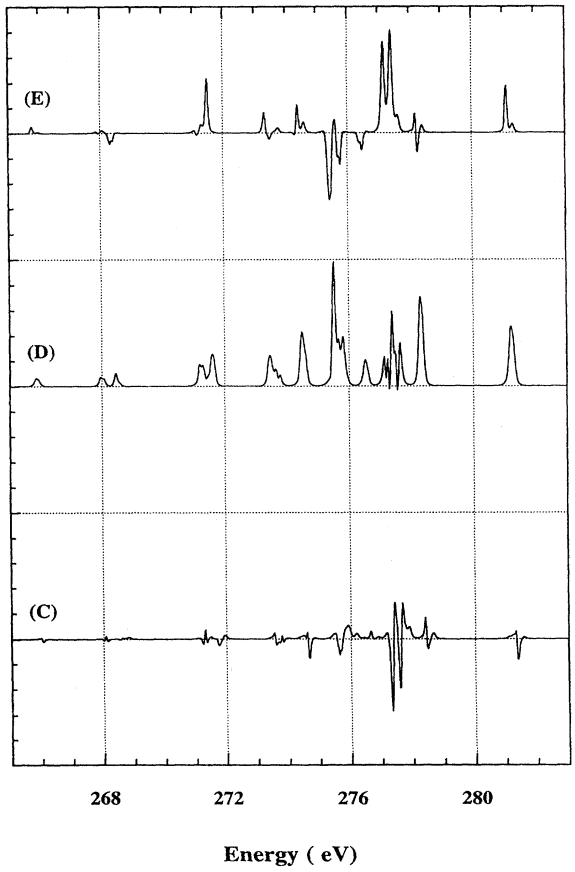

FIG. 8. Differences of the calculated spectra for aniline from one- and two-step models. The parameters are the same as used for Figs. 6 and 7.

case, we feel that we tentatively can give some statements on the role of chemical shifts for RIXS spectra in general. If we consider cases with small, intermediate, and large shifts, we find the RIXS technique to be informative in the first and the third of these cases. For large shifts, say above 1 eV, the core level can be selectively excited, and the corresponding RIXS spectra can be analyzed in terms of electronic structure theory, local intensity rules, etc., for the particular core site. For very small shifts, below 0.5 eV, the interference effects will make RIXS spectra crucially dependent on the precise value of the shifts, and can make it possible to assign shifts although they remain nonresolved in the corresponding absorption spectrum. In the intermediate region, outside the region of strong interference, but still nonresolved in absorption, the RIXS spectra will overlap in a way that makes it difficult to distinguish the shifts. They will furthermore be Raman shifted with respect to each other in such cases. Precise limits of these regions will of course be set by the degree of vibrational excitations, the core hole state lifetime, and the form of the excitation energy function.

Further information from chemically shifted RIXS spectra of the kind presented here will be provided by polarization or angular-dependent measurements, since the polarization anisotropy is very sensitive to interference effects [7]. In addition to the previously established band conserving and symmetry selective character, the site selectivity opens new possibilities for geometric and electronic structure investigations by means of resonance x-ray spectroscopy.

ACKNOWLEDGMENTS

This work was supported by Cray Research Inc. and the Swedish Natural Science Research Council (NFR) and the Göran Gustafssons Foundation for Research in Natural Science and Medicine. We would like to thank T. Warwick, P. Henemann, E. Rotenberg, and J. D. Denlinger for the assistance during the measurements. The work at ALS, Lawrence Berkeley Laboratory was supported by the director, Office of Energy Research, Office of Basic Energy Science, Material Sciences Division of the U.S. Department of Energy, under Contract No. DE-AC03-76SF00098.

[1] A. Lindh and O. Lundquist, Arkiv Mat. Astron. Fysik **18**, (1924).
[2] R. Manne, in *Inner-shell and X-ray Physics of Atoms and Solids*, edited by D. J. Fabian *et al.* (Plenum Press, New York, 1981).
[3] T. Warwick, P. Heineman, D. Mossessian, and H. Padmore, in *International Conference on Synchrotron Radiation Instruments* (Stony Brook, New York, 1994).
[4] J. Nordgren, G. Bray, S. Cramm, R. Nyholm, J. E. Rubensson, and N. Wassdahl, Rev. Sci. Instrum. **60**, 1690 (1989).
[5] F. Kh. Gel'mukhanov and H. Ågren, Phys. Rev. A **49**, 4378 (1994).
[6] Y. Luo, H. Ågren, and F. K. Gelmukhanov, J. Phys. B **27**, 4169 (1994).
[7] Y. Luo, H. Ågren, F. Kh. Gelmukhanov, J. H. Guo, P. Skytt, N. Wassdahl, and J. Nordgren, Phys. Rev. B (to be published).
[8] H. Ågren, V. Carravetta, O. Vahtras, and L. G. M. Pettersson, Chem. Phys. Lett. **222**, 75 (1994).
[9] H. J. Aa. Jensen and H. Ågren, Chem. Phys. **104**, 229 (1986).
[10] P. Glans, R. LaVilla, Y. Luo, H. Ågren, and J. Nordgren, J. Phys. B **27**, 3399 (1994).
[11] J. H. Guo, P. Skytt, N. Wassdahl, J. Nordgren, Y. Luo, O. Vahtras, and H. Ågren, Chem. Phys. Lett. **235**, 152 (1995).
[12] M. Tronc, G. C. King, and H. Read, J. Phys. B **12**, 137 (1979).
[13] J. J. Sakurai, in *Advanced Quantum Mechanics* (Addison-Wesley, Reading, Mass., 1967).
[14] F. Kh. Gel'mukhanov and H. Ågren, Phys. Rev. A **50**, 1129 (1994).
[15] Y. Luo *et al.* (unpublished).
[16] J. Nordgren, L. Selander, L. Pettersson, R. Brammer, M. Bäckström, C. Nordling, and H. Ågren, Chem. Phys. **84**, 333 (1984).
[17] A. P. Hitchcock, M. Pocock, C. E. Brion, M. S. Banna, D. C. Frost, C. A. McDowell, and B. Wallbank, J. Electron. Spectrosc. **13**, 345 (1978).
[18] J. A. Horsley, J. Stöhr, A. P. Hitchcock, D. C. Newbury, A. L. Johnson, and F. Sette, J. Chem. Phys. **83**, 6099 (1985).
[19] P. Yannoulis, R. Dudde, K. H. Frank, and E. E. Koch, Surf. Sci. **189/190**, 519 (1987).
[20] P. Skytt, J. H. Guo, N. Wassdahl, J. Nordgren, Y. Luo, and H. Ågren, Phys. Rev. A **52**, 3572 (1995).
[21] H. Ågren, and P. S. Bagus, J. Am. Chem. Soc. **107**, 134 (1984).
[22] K. Siegbahn, C. Nordling, G. Johansson, J. Hedman, P. F. Hedén, K. Hamrin, U. Gelius, T. Bergmark, L. O. Werme, R. Manne, and Y. Baer, *ESCA Applied to Free Molecules* (North-Holland, Amsterdam, 1969).
[23] J. L. Solomon, R. J. Madix, and J. Stöhr, Surf. Sci. **255**, 12 (1991).
[24] A. Naves de Brito, N. Correia, S. Svensson, and H. Ågren, J. Chem. Phys. **95**, 2965 (1991).